Seismic geomorphology: imaging elements of depositional systems from shelf to deep basin using 3D seismic data: implications for exploration and development

HENRY W. POSAMENTIER
Anadarko Canada Corporation, 425 1st Street SW, Calgary, Alberta T2P 4V4, Canada
(e-mail: henry_posamentier@anadarko.com)

Abstract: 3D seismic data can play a vital role in hydrocarbon exploration and development especially with regard to mitigating risk associated with presence of reservoir, source, and seal facies. Such data can afford direct imaging of depositional elements, which can then be analyzed using seismic stratigraphy and seismic geomorphology to yield predictions of lithologic distribution, insights to compartmentalization, and identification of stratigraphic trapping possibilities. Benefits can be direct, whereby depositional elements at exploration depths can be identified and interpreted, or they can be indirect, whereby shallow-buried depositional systems can be clearly imaged and provide analogues to deeper exploration or development targets. Examples of imaged depositional elements from both shallow and deep sections are presented.

Seismic data have long been used for lithologic prediction. Initially, such interpretations were based on the analysis of 2D seismic reflection profiles (Vail *et al.* 1977). The approach that was used involved first the identification of reflection terminations (e.g. onlap, downlap, toplap, erosional truncation) and the recognition of stratigraphic discontinuities such as unconformities. Second, the reflection geometries between discontinuity surfaces were described (e.g., oblique or sigmoidal progradation). Finally, the amplitude, continuity and frequency of reflections were described and mapped. In sum, these observations yielded insights with regard to the type of depositional systems present. This approach was referred to as seismic stratigraphy (Vail *et al.* 1977).

With the development of 3D seismic acquisition techniques, the opportunity to image geological features in map view opened up new approaches to geological prediction (e.g. Weimer & Davis 1996). Various reflection attributes such as amplitude, dip magnitude, dip azimuth, time/depth structure and curvature, to name a few, can be observed to yield direct images of depositionally and structurally significant features. In addition, analysis of seismic intervals can lend further insight to such features. The study of depositional systems using 3D-seismic derived images has been referred to as *seismic geomorphology* (Posamentier 2000). This represents a significant step change in how seismic interpreters evaluate 3D seismic data. In general, depositional environments had commonly been inferred on the basis of cross-section derived stratigraphic architecture and subsequent mapping of seismic facies leading to lithologic predictions. With the advent of seismic geomorphology, discrete, detailed depositional subenvironments and depositional elements could be interpreted directly from map view images leading to much more accurate understanding of lithologic distribution patterns and enhanced prediction of the distribution of reservoir, source and seal facies.

The following discussion will be divided into two parts, the first section illustrating examples of seismic images of depositional elements at exploration depths, and the second illustrating images of depositional elements at shallow depths.

Depositional elements at exploration depths

Cretaceous channels—Alberta, Canada

Figure 1 illustrates two views of a major channel crosscut by two lesser channels. Figure 1A is a *horizon slice* or *flattened time slice*, whereby a reflection 32 ms above was interpreted and used as a reference horizon for the purpose of slicing through the 3D seismic volume. Figure 1B is a reflection amplitude map of reflections immediately below the reflection associated with the channel. Each images the channels in a different way, with different details brought out by the two display styles. Both show linear features within the large channel, which can be interpreted as possible point bar deposits. Both show a crosscutting and therefore younger channel in the middle of the illustration. However Figure 1A shows another smaller channel crosscutting the larger channel towards the bottom of the illustration, not apparent in Figure 1B.

The integration of seismic geomorphology and seismic stratigraphy is illustrated in Figure 2. Inclined reflections within the interpreted channel fill can be observed on the reflection profile oriented normal to the long axis of the large channel (Fig. 2B). These reflections can be interpreted to represent lateral accretion surfaces associated with point bar deposition within the channel (Figs 2C and D). The isopach map indicates the presence of a thicker channel fill on the southwestern side of the channel (Figs 2A and D). The seismic profile reveals that the thicker part of the channel does not correspond to a deeper channel thalweg, but rather is associated with a 'bump' across part of the channel. This 'bump' is interpreted to be associated with a substrate that is less compactible than the other part of the channel fill (Fig. 2C). This least compactible section would suggest the presence of lateral accretion sets that would be most sand-rich, sand being less compactible than silt or shale (Fig. 2D).

Planning of horizontal well bore trajectories should take into account the presence of internal stratigraphic architecture comprising varying lithologies (Fig. 3). In this instance, orientation of horizontal well bores parallel to the lateral accretion deposits would allow for improved reservoir management. Lithologic variations associated with bedding parallel boreholes would be lower than those associated with bedding normal boreholes. Consequently, drilling parallel to bedding planes might better protect against gas or water breakthrough. Alternatively, if gas or water breakthrough is not a concern, then a preferred strategy might be to drill across bedding planes so as to access and drain multiple compartments with a single borehole.

Several crosscutting Cretaceous-aged channels are illustrated in Figure 4. This image represents a map of the negative polarity total amplitudes within a 16 ms window that contains at

DAVIES, R. J., CARTWRIGHT, J. A., STEWART, S. A., LAPPIN, M. & UNDERHILL, J. R. (eds) 2004. *3D Seismic Technology: Application to the Exploration of Sedimentary Basins*. Geological Society, London, Memoirs, **29**, 11–24. 0435-4052/04/$15

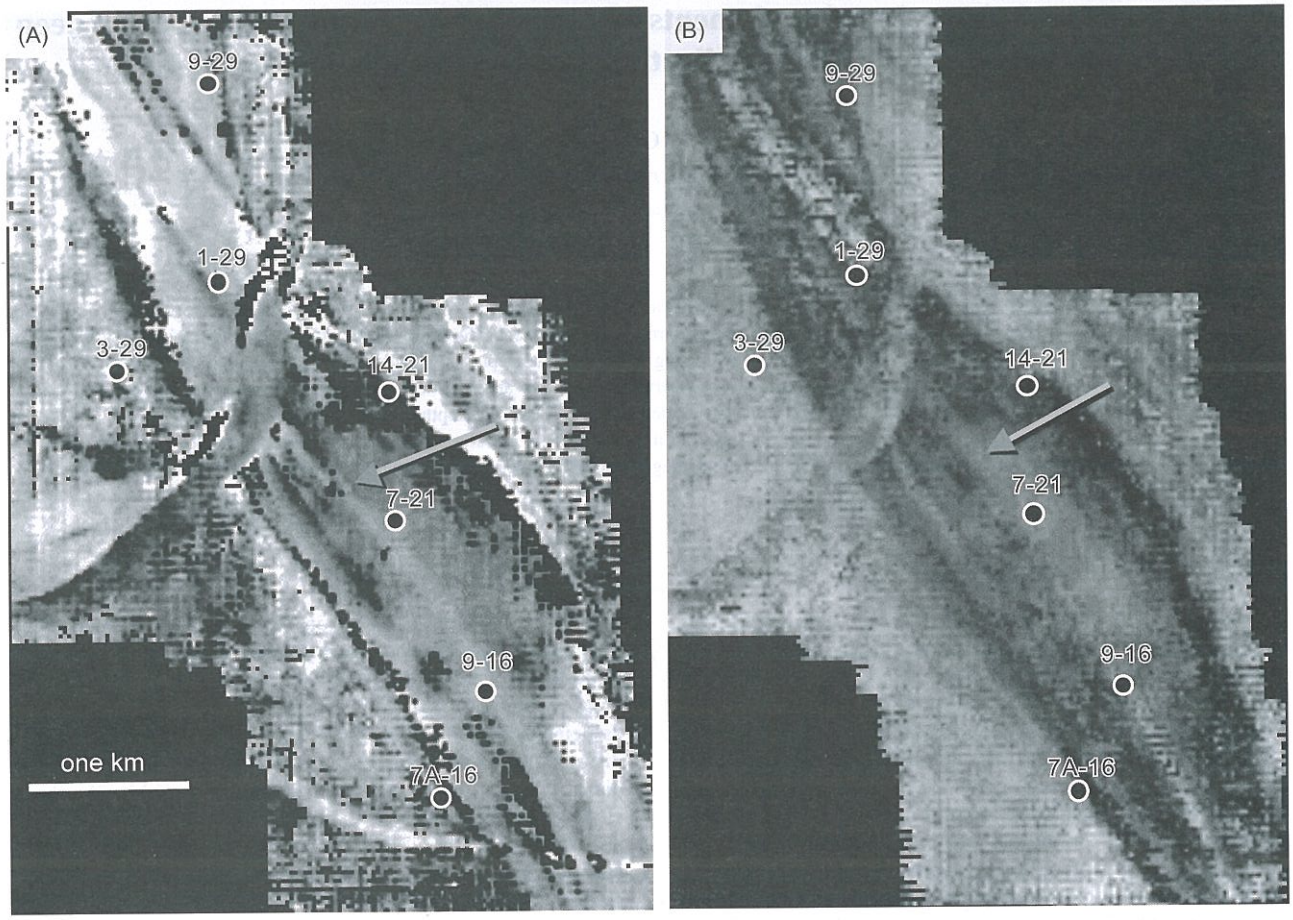

Fig. 1. Cretaceous fluvial/estuarine channel. (**A**) map of the amplitude of the reflection peak immediately underlying the top of the channel. (**B**) map of an amplitude extract at a level 32 ms below a regional horizon (i.e., horizon slice). Two younger crosscutting channels can be observed. The linear pattern within the channel (arrow) suggests the presence of lateral accretion in association with the development of alternate or point bars.

least eight generations of crosscutting channels. Figure 5 illustrates two additional images of this same geological section; note that each image brings out different aspects of these channels. Figure 6 illustrates section views through some of these channels. Note that interpretation of such profiles alone, in the absence of 3D seismic coverage would have yielded a significantly inferior geological interpretation. The presence of lateral accretion deposits, clearly imaged on the map view image are only dimly recognizable as such on the reflection profile. Nonetheless, the integration of the map view with the section view images yields a more robust geological interpretation, which ultimately can be applied to exploration and development issues.

Fluvial systems characterized by high-sinuosity channel belts are illustrated in Figures 7 and 8. The concentric arcs imaged in map view represent sections through point bar deposits and may represent scroll bars. Figure 7 illustrates an analogous modern feature from the Mississippi floodplain for comparison. Examination of the reflection profile shown in Figure 8 illustrates a stratigraphic representation of such deposits; interpretation of the correct depositional element would likely not have been possible if only the reflection profile were available.

Fluvial systems overlying a major unconformity surface are illustrated in Figures 9–11. In this instance, Cretaceous fluvial channel fill deposits directly overlie Mississippian-aged carbonates. Figure 9 shows several co-rendered horizon attributes as well as a seismic profile illustrating the stratigraphic discontinuity between Cretaceous-aged and Mississippian-aged deposits. Each image portrays the depositional elements somewhat differently. Co-rendering of different attributes also can serve to enhance the features in question (Fig. 9). In certain instances perspective views can provide a deeper appreciation for the 'lay of the land' (Figs 10 and 11). Note the apparent dendritic drainage pattern off the highland area at the right side of Figure 10.

Shallow-marine shelf ridges—offshore northwest Java, Indonesia

Numerous linear seismic reflection amplitude anomalies are observed on horizon slices in the Miocene section offshore northwest Java, Indonesia (Figs 12 and 13). These features have been interpreted as tidal current related shallow marine shelf ridges (Posamentier 2002*a*). The well-log cross section (Fig. 14) illustrates an abrupt sandstone pinchout towards the west, in the inferred direction of wave migration. This pinchout is expressed seismically as a sharp linear boundary (Fig. 13). In contrast the trailing edges of these shelf ridges are expressed as less well-defined amplitude changes (Fig. 13). Posamentier (2002*a*) has shown that these pinchouts can define a stratigraphic trapping component.

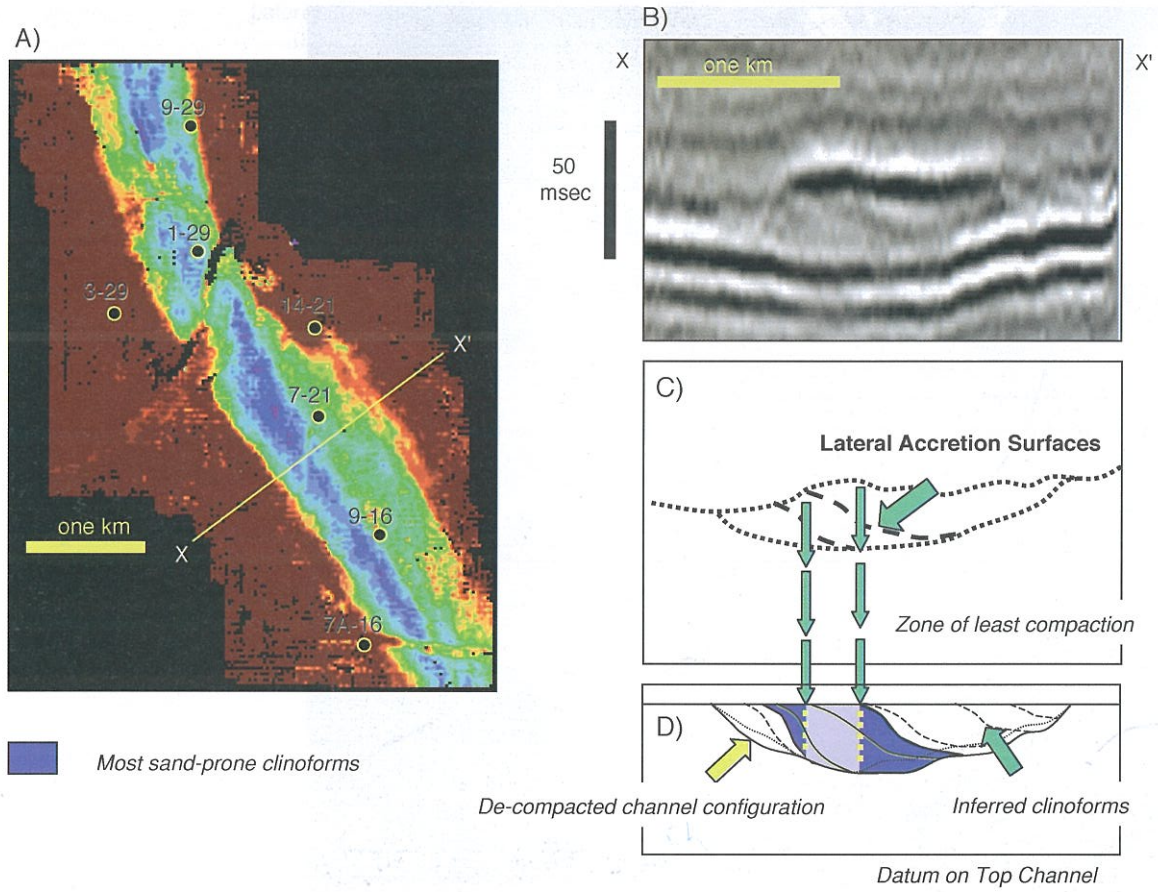

Fig. 2. (**A**) Isopach map of channel fill for same channel shown in Figure 1. Blue colour indicates maximum thickness of 31 m; red colour indicates zero thickness. (**B**) Seismic reflection profile oriented transverse to channel axis. Irregularity of upper bounding surface indicates effects of differential compaction of channel fill. (**C**) Geological interpretation of seismic reflection profile shown in (A). Note presence of lateral accretion surfaces. (**D**) Illustrates de-compacted transverse profile of channel fill. Least compactible lateral accretion wedges are highlighted in blue.

Basement—Alberta, Canada

In certain instances, where basement reflections are well defined, subcrop seismic expression can provide significant insight with regard to basement lithologies. Figure 15 illustrates subcrop seismic amplitude expression indicative of likely metamorphic basement. These horizon slices and amplitude extractions shown here illustrate styles of deformation that commonly characterize metamorphic terrains.

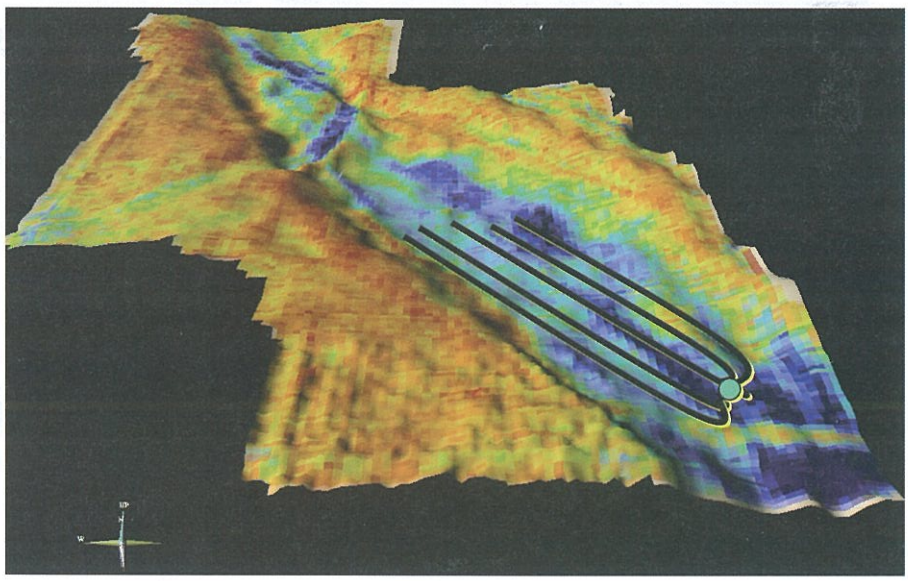

Fig. 3. Amplitude of seismic reflection at upper bounding surface of channel fill shown in Figs 1 and 2 draped onto perspective view of base channel seismic reflection. Approximate location of horizontal borehole trajectories are shown.

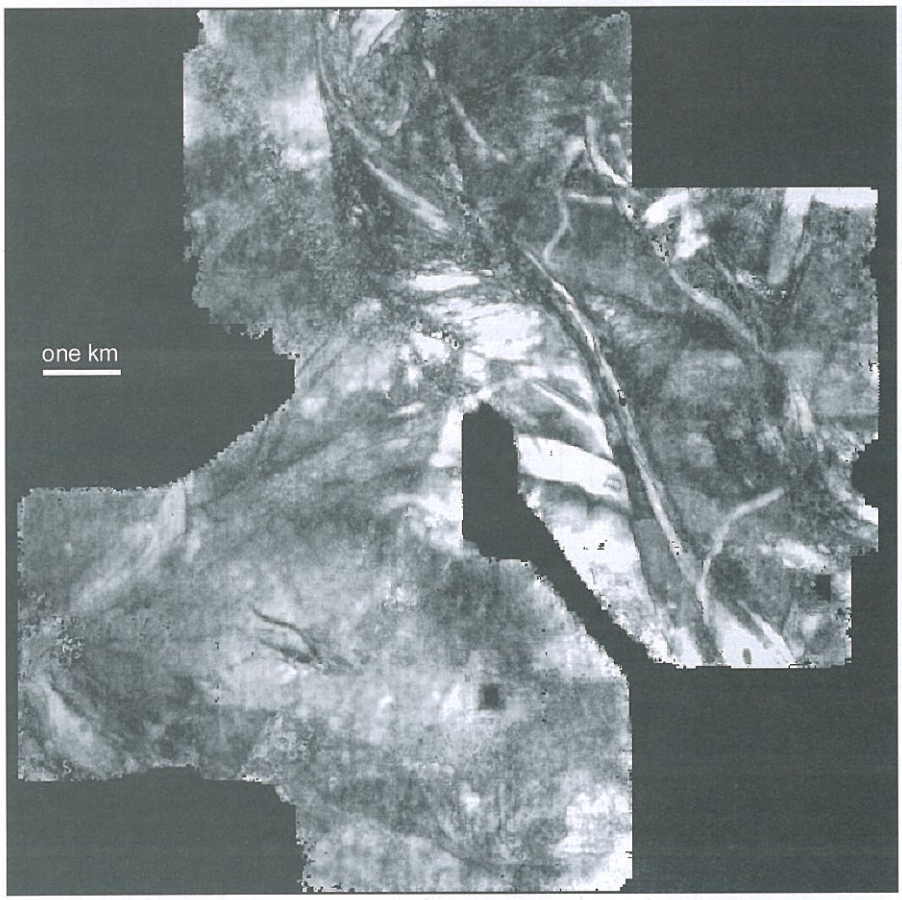

Fig. 4. Negative polarity total amplitude of 16 ms thick seismic interval bracketing a fluvial/deltaic depositional environment. Crosscutting channels give indication of temporal relationships; eight discrete levels of channels can be observed.

Depositional elements at shallow burial depths

The study of seismic data within uppermost stratigraphic sections (i.e. within the upper 0.5 to 1.5 seconds of data) can yield significant insight to preserved depositional elements in both shallow and deep depositional environments (Posamentier 2000; Posamentier *et al.* 2000). These potentially well-imaged features can serve as useful analogues for deeper exploration and development targets, where similar depositional elements are known to exist. Both deep-water as well as shallow water depositional environments can be analyzed this way.

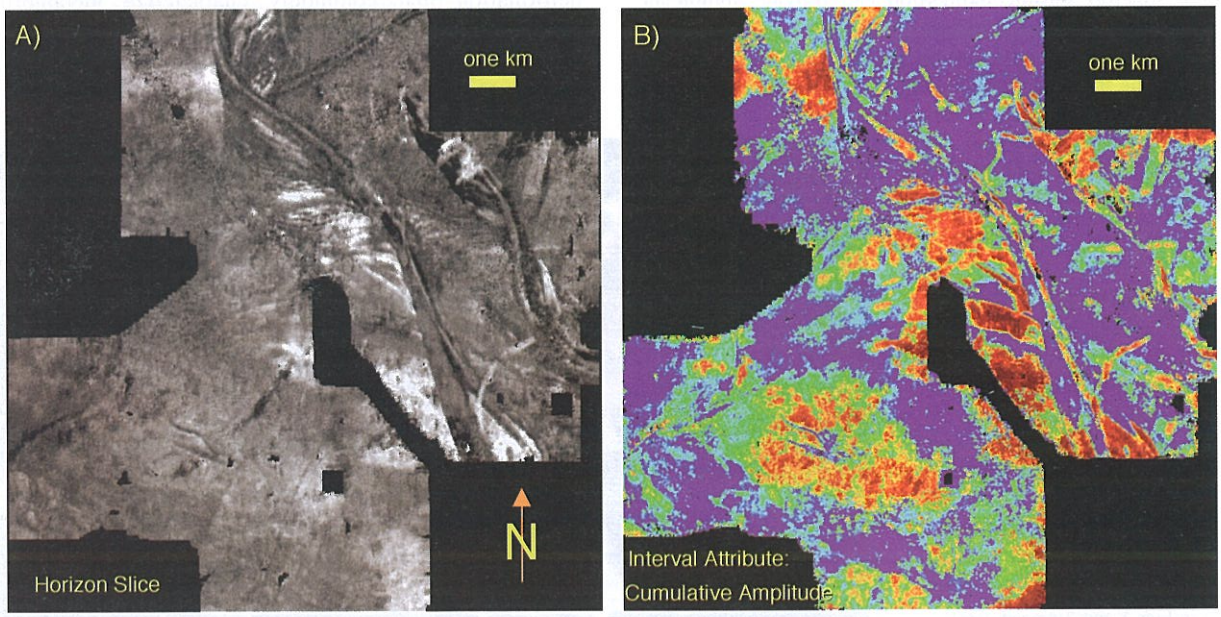

Fig. 5. (**A**) Horizon slice through upper part of 16 ms interval shown in Figure 4. Channel in centre of image characterized by northward-directed lateral accretion suggesting paleo-flow direction from southeast to northwest. (**B**) Cumulative amplitude map of same 16 ms interval shown in Figure 4. Hydrocarbon and lithological effects are accentuated.

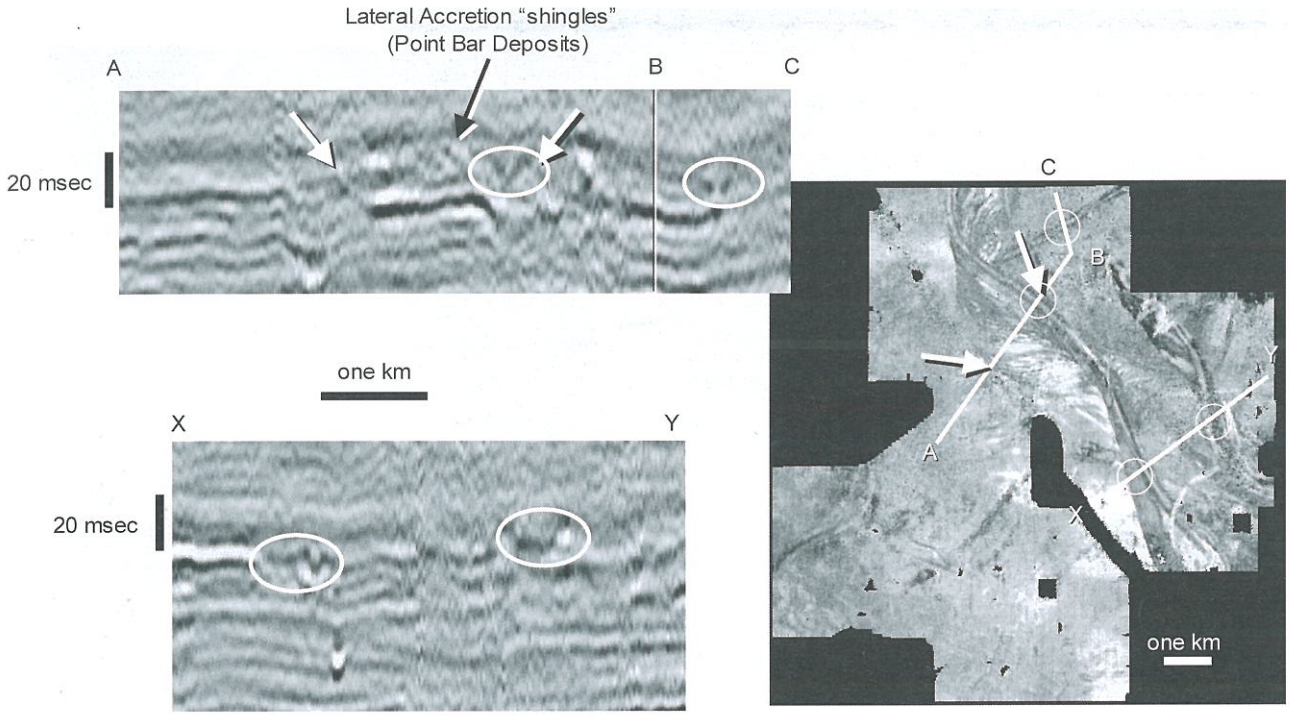

Fig. 6. Two transverse seismic profiles across channels shown in Figure 5A. Note the 'shingled' stratigraphic expression of point bar deposits observed in Figure 5A.

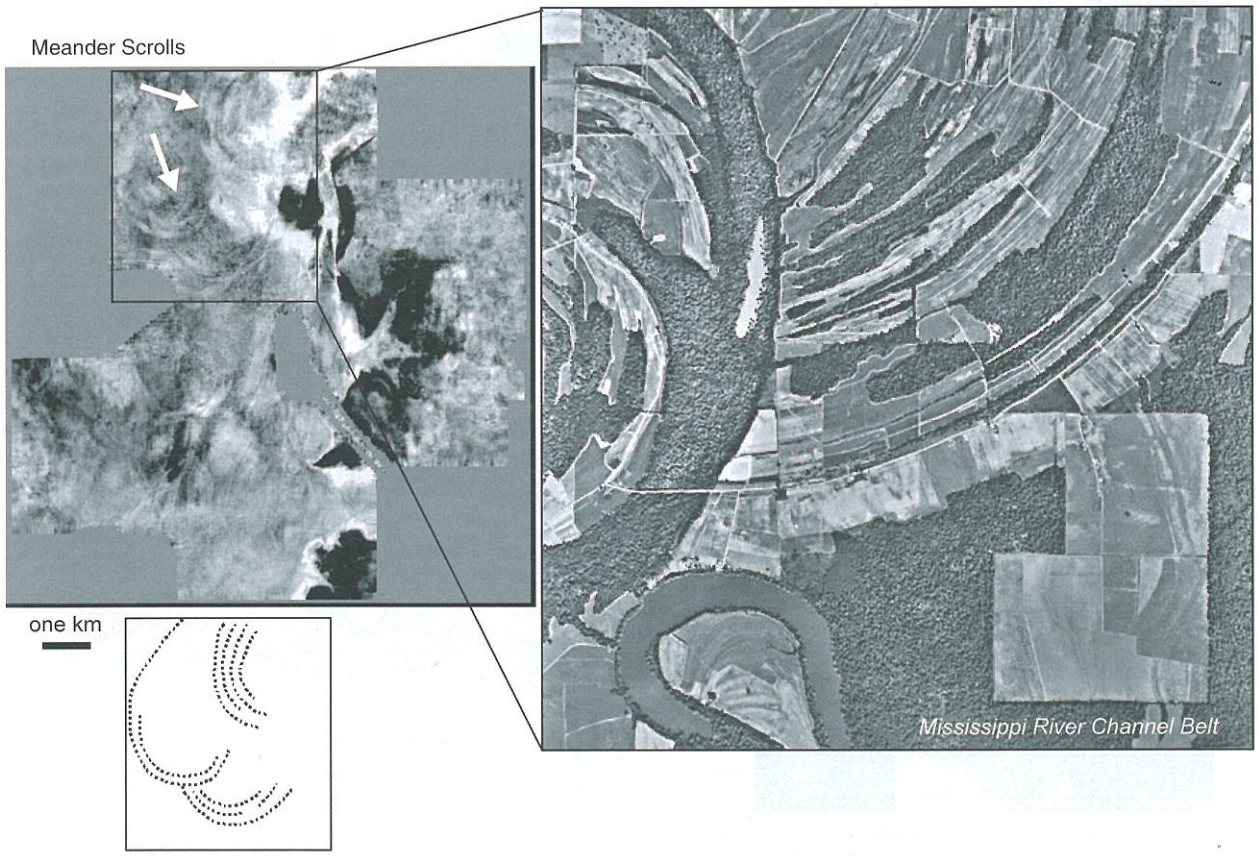

Fig. 7. Horizon slice through non-marine section illustrating seismic geomorphologic expression of meander loops. Inset illustrates Mississippi River modern analogue.

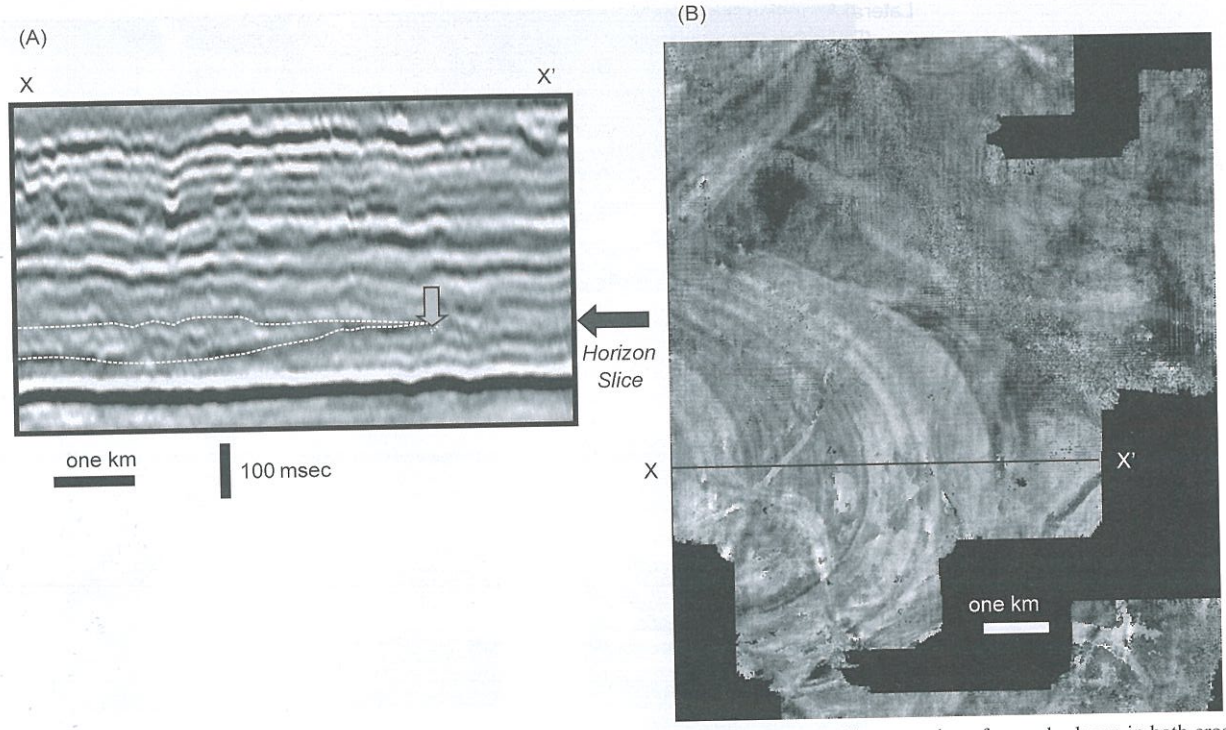

Fig. 8. Horizon slice through non-marine section illustrating seismic geomorphologic and stratigraphic expression of meander loops in both cross section (**A**) as well as plan view (**B**).

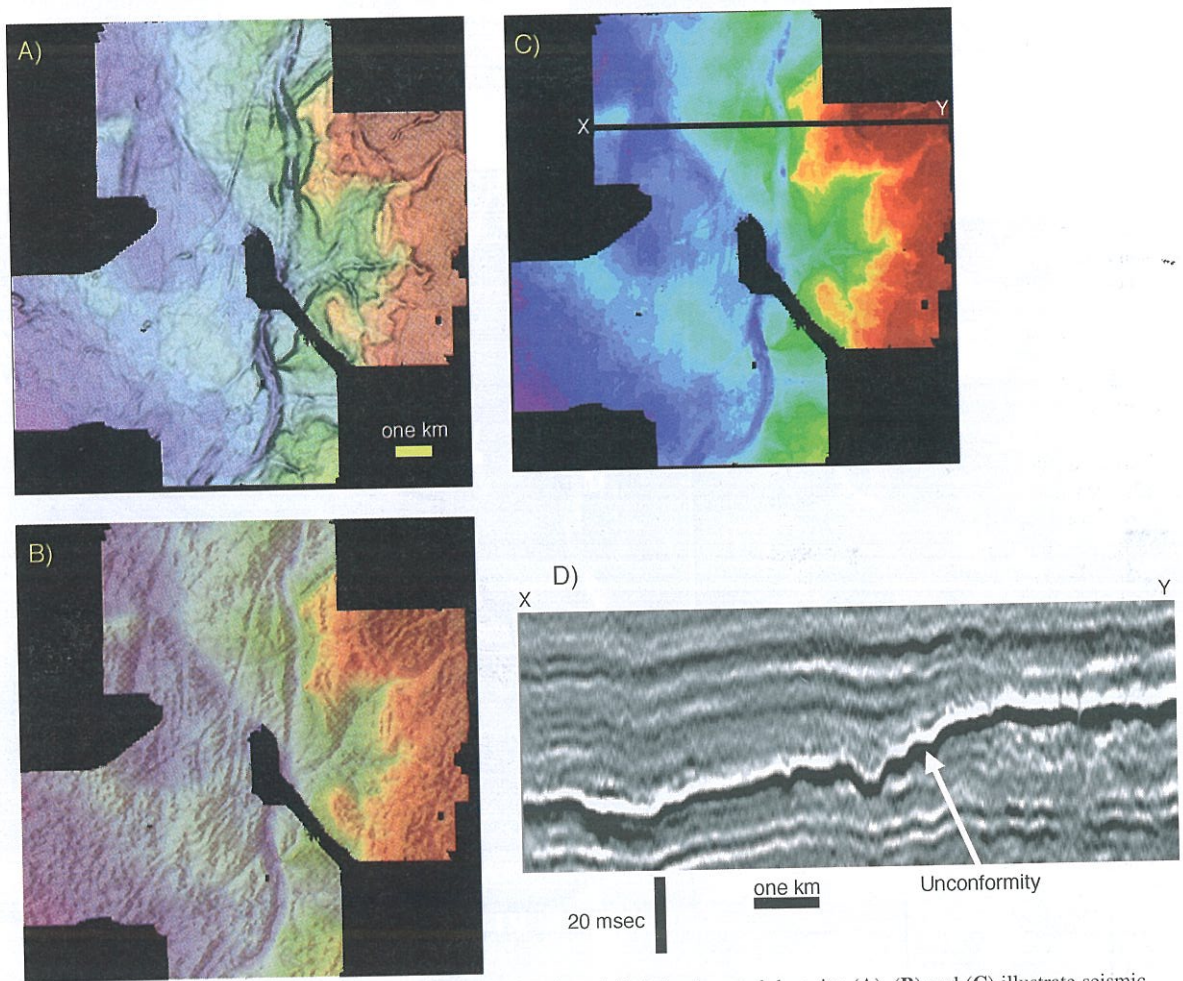

Fig. 9. Several images of unconformity separating Cretaceous-aged from Mississippian aged deposits. (**A**), (**B**) and (**C**) illustrate seismic geomorphological expression of this surface, whereas (**D**) illustrates the seismic stratigraphic expression of the same surface. This unconformity surface is characterized by the presence of numerous channels evident both in map as well as section view. (**A**) Co-rendered dip magnitude and time structure. (**B**) Co-rendered dip azimuth and time structure. (**C**) Time structure. (**D**) Seismic profile.

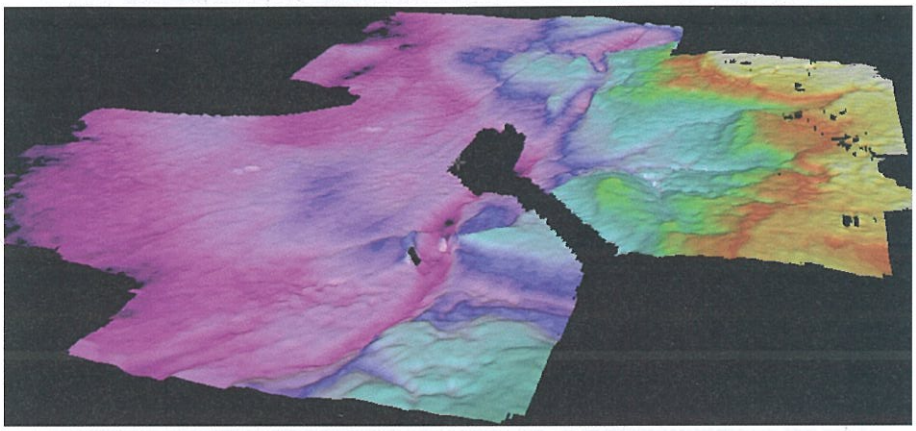

Fig. 10. Perspective view of unconformity separating Cretaceous-aged from Mississippian aged deposits, shown in Figure 9.

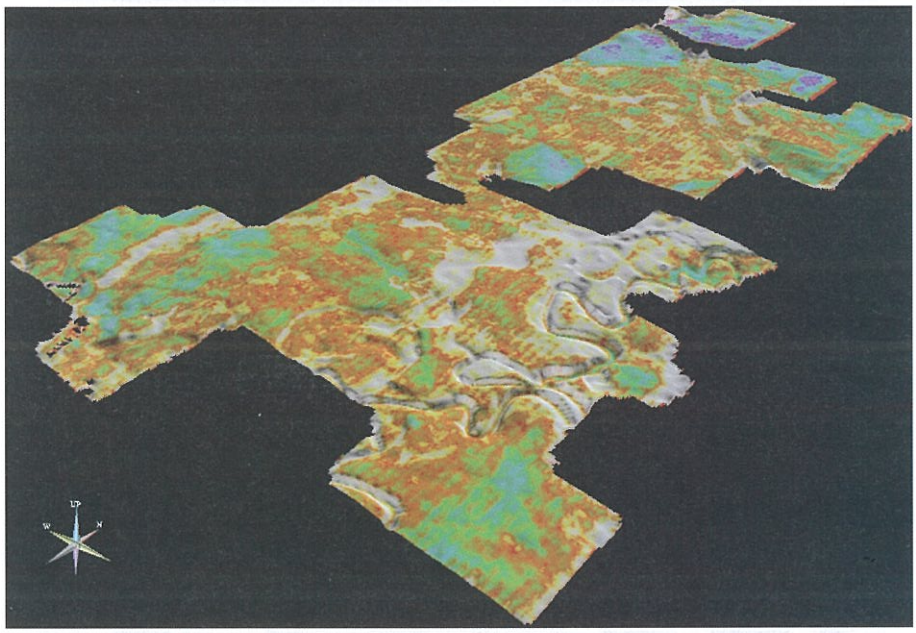

Fig. 11. Perspective view of unconformity separating Cretaceous-aged from Mississippian aged deposits. High sinuosity incised channel can be observed on this surface.

Deep-water depositional environments

Shallow-buried, deep-water deposits can be readily imaged in great detail. Such detailed images provide useful analogues for more deeply buried systems. Figure 16 shows a moderate to high sinuosity channel deposited on the basin floor during the late Pleistocene (Posamentier *et al.* 2000). The upper bounding surface of this channel-levee system lies approximately 80–100 m below the sea floor. Two attributes of this surface are shown: dip azimuth (Fig. 16A) and dip magnitude (Fig. 16B). The dip azimuth map has the appearance of a shaded relief map and from it the various geomorphic elements, such as the channel, the levee crests, and overbank sediment wave fields can be interpreted. The dip magnitude map accentuates those features that are characterized by steeper slopes. In this instance, the dip magnitude map can be used to identify the larger sediment waves that lie adjacent to outer meander bends (Fig. 16B). From an exploration perspective, the sediment wave fields that are characterized by steeper flanks are inferred to be more sand prone than those with more gentle slopes. Moreover, the distribution of these sandstones will have a preferred orientation, i.e. parallel to the waves' long axes, a characteristic potentially important from a field development perspective.

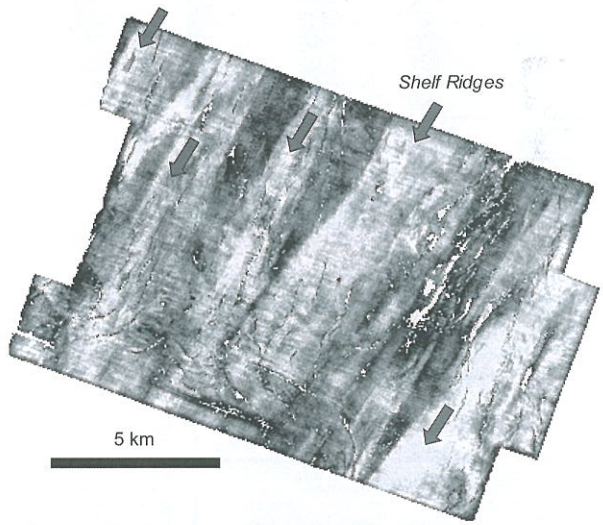

Fig. 12. Amplitude extraction from seismic horizon slice illustrating linear trending shelf ridges of Miocene age, offshore northwest Java, Indonesia.

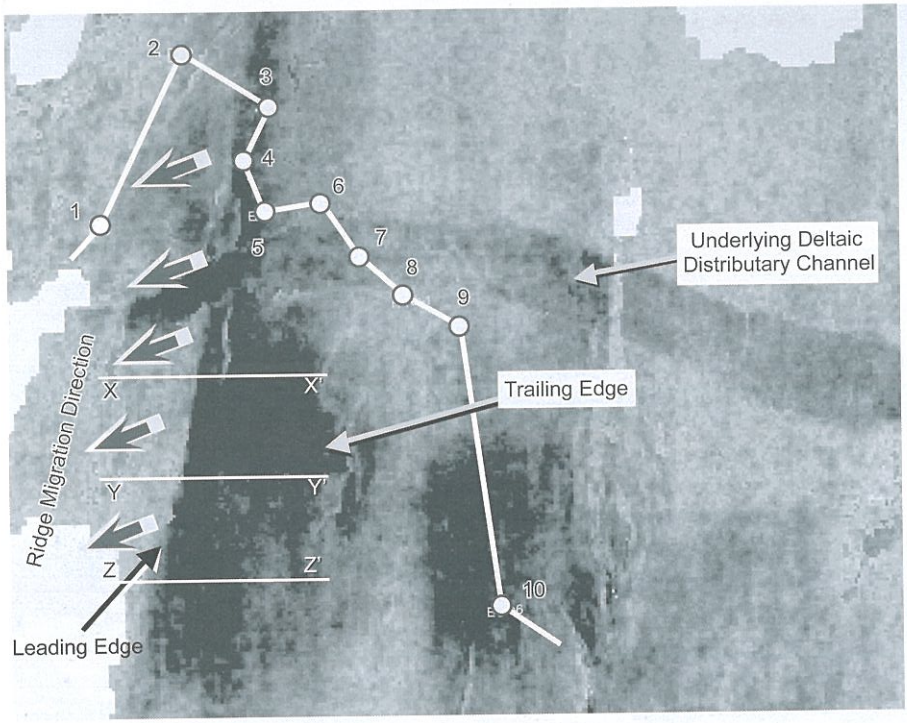

Fig. 13. Amplitude extraction from seismic horizon slice illustrating shelf ridge of Miocene age, offshore northwest Java, Indonesia. Ridge migration direction is inferred to be towards the southwest. The leading edge is characterized by a sharp linear boundary whereas the trailing edge boundary is less well defined. The channel feature that appears on this image lies at a lower stratigraphic level (see Fig. 14).

The evolution of sinuous turbidity flow channels can be observed in Figure 17. This horizon slice illustrates the progressive down-system meander loop migration (i.e. 'sweep') as well as a minor degree of meander loop expansion (i.e. 'swing') that commonly characterizes such systems (Peakall *et al.* 2000).

Another high-sinuosity channel-levee system is shown in Figure 18. The 3D perspective view (Figs 18A and C) as well as the seismic profile (Fig. 18B) illustrate the effects of differential compaction in this type of environment. The presence of relatively less compactable sand within the channel results in an inversion of topography after deposition. The top of the channel

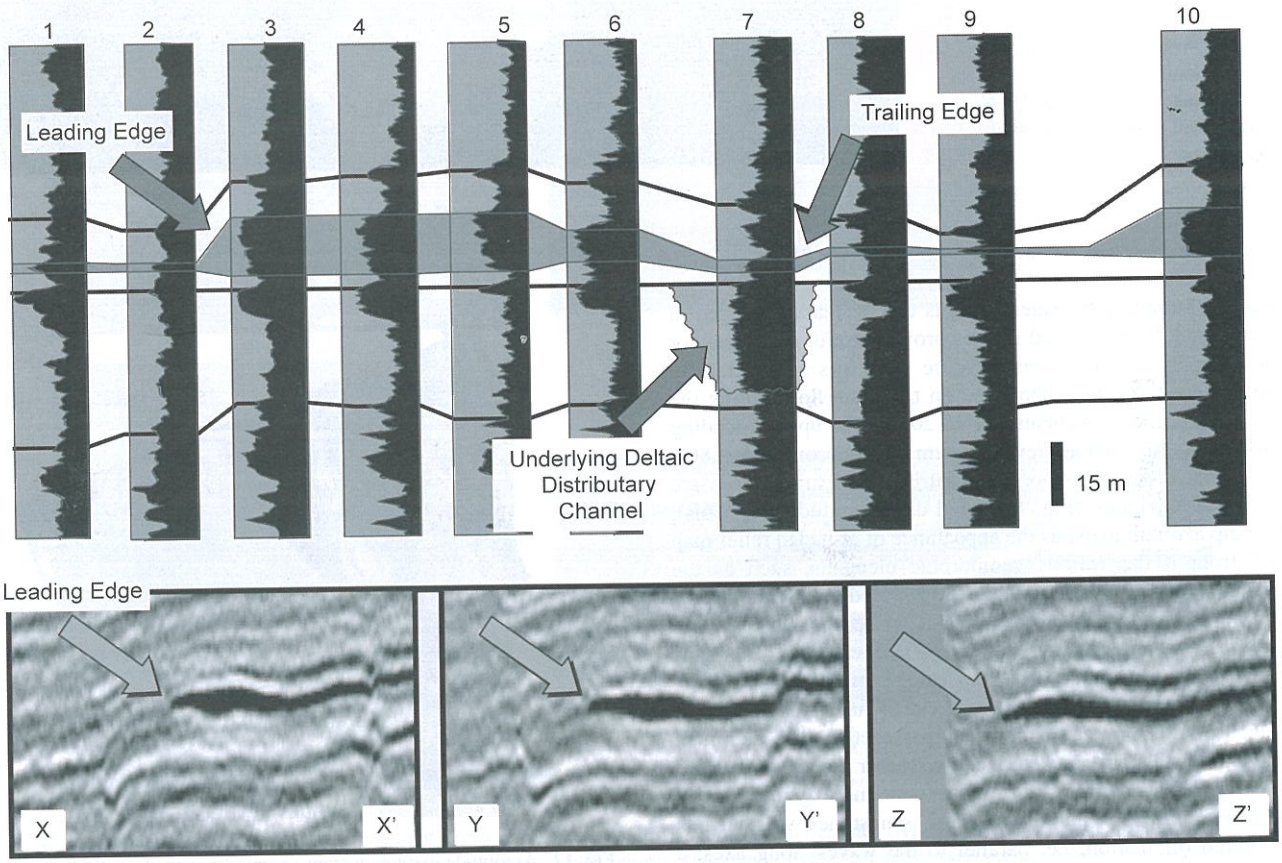

Fig. 14. Well log cross section and seismic profiles across the shelf ridge shown in Figure 13. The sand pinches out abruptly at the leading edge, between wells 2 and 3. The locations of the well log cross section and the seismic profiles are shown in Figure 13.

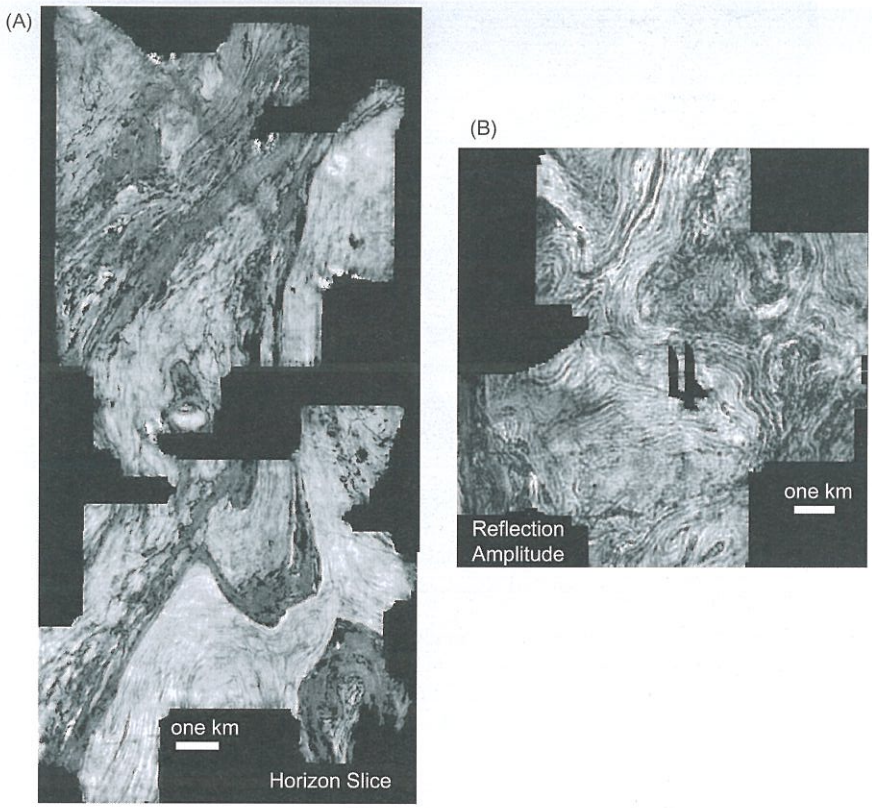

Fig. 15. Two images of basement in the western Canada sedimentary basin, Alberta, Canada. (**A**) Horizon slice and (**B**) amplitude extraction from basement reflection.

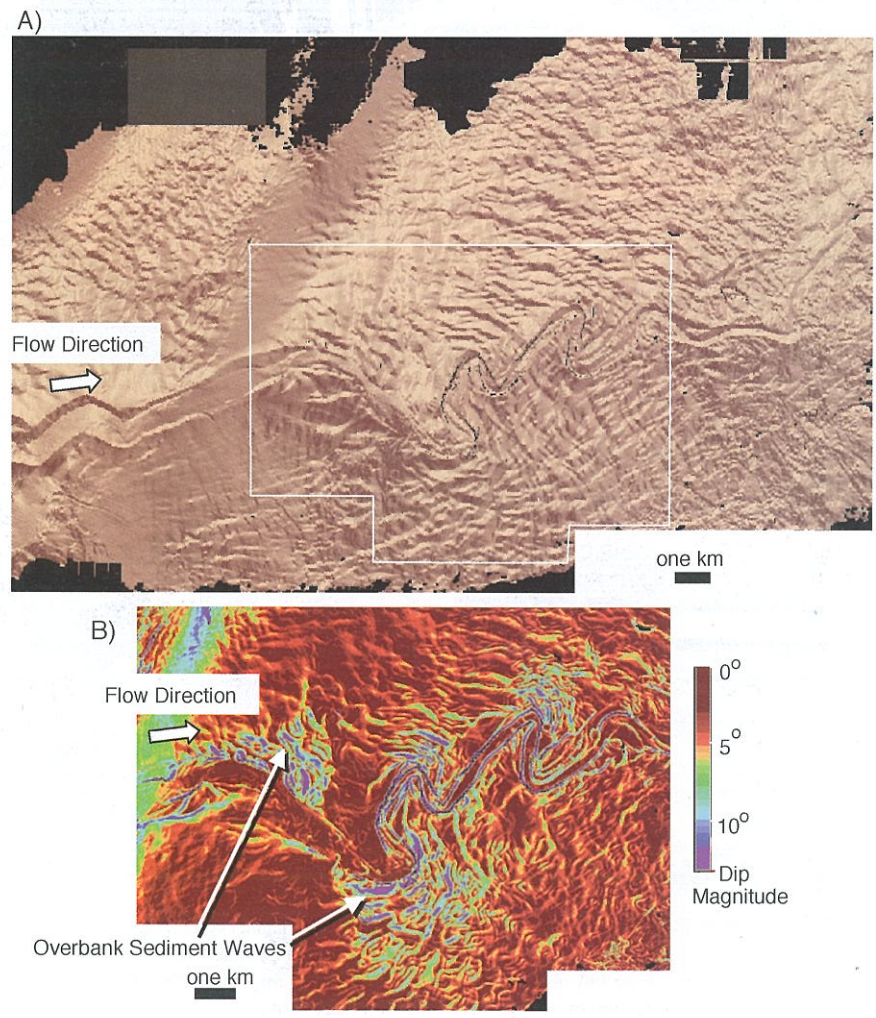

Fig. 16. Dip azimuth (**A**) and dip magnitude (**B**) maps of top of deep-water channel-levee complex offshore Borneo, Indonesia. The dip magnitude image illustrates a simulated relief map with lighting from the north. Numerous overbank sediment waves on either side of the channel can be observed. The dip magnitude map highlights the higher relief, steeper-flanked sediment waves.

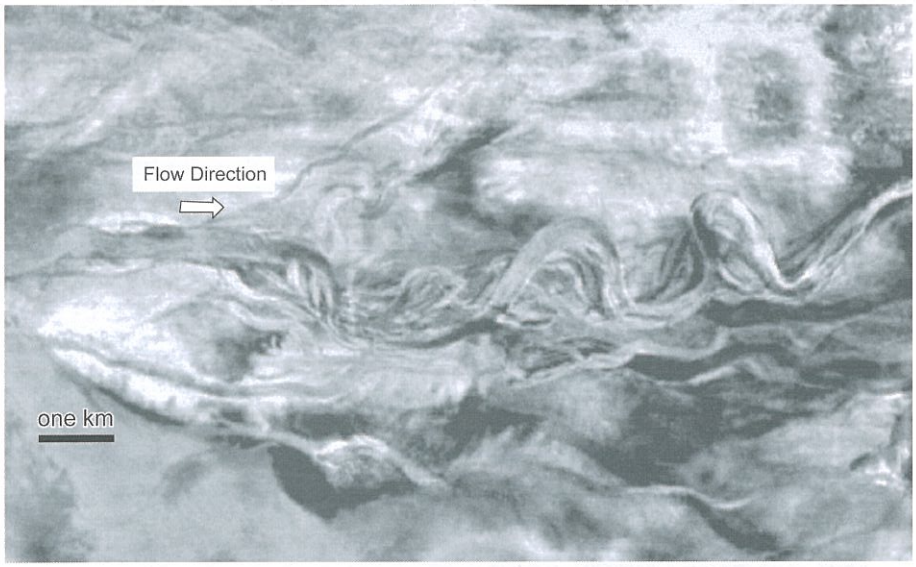

Fig. 17. Horizon slice amplitude extraction illustrating a high-sinuosity deep-water leveed channel. This channel is characterized by extensive meander loop expansion as well as down-system meander loop migration.

fill likely was somewhat lower than the surrounding floodplain at the time of deposition; however, because of the greater sand content of the channel fill relative to the adjacent floodplain, the floodplain compacted more and resulted in the development of a post-depositional 'channel ridge'.

A linked shelf edge and deep-water environment is illustrated in Figure 19. The dip-oriented seismic profile (Fig. 20) illustrates a shelf edge deltaic system characterized by both forced regression as well as normal regression. The transverse-oriented seismic profiles (Fig. 21) illustrate the

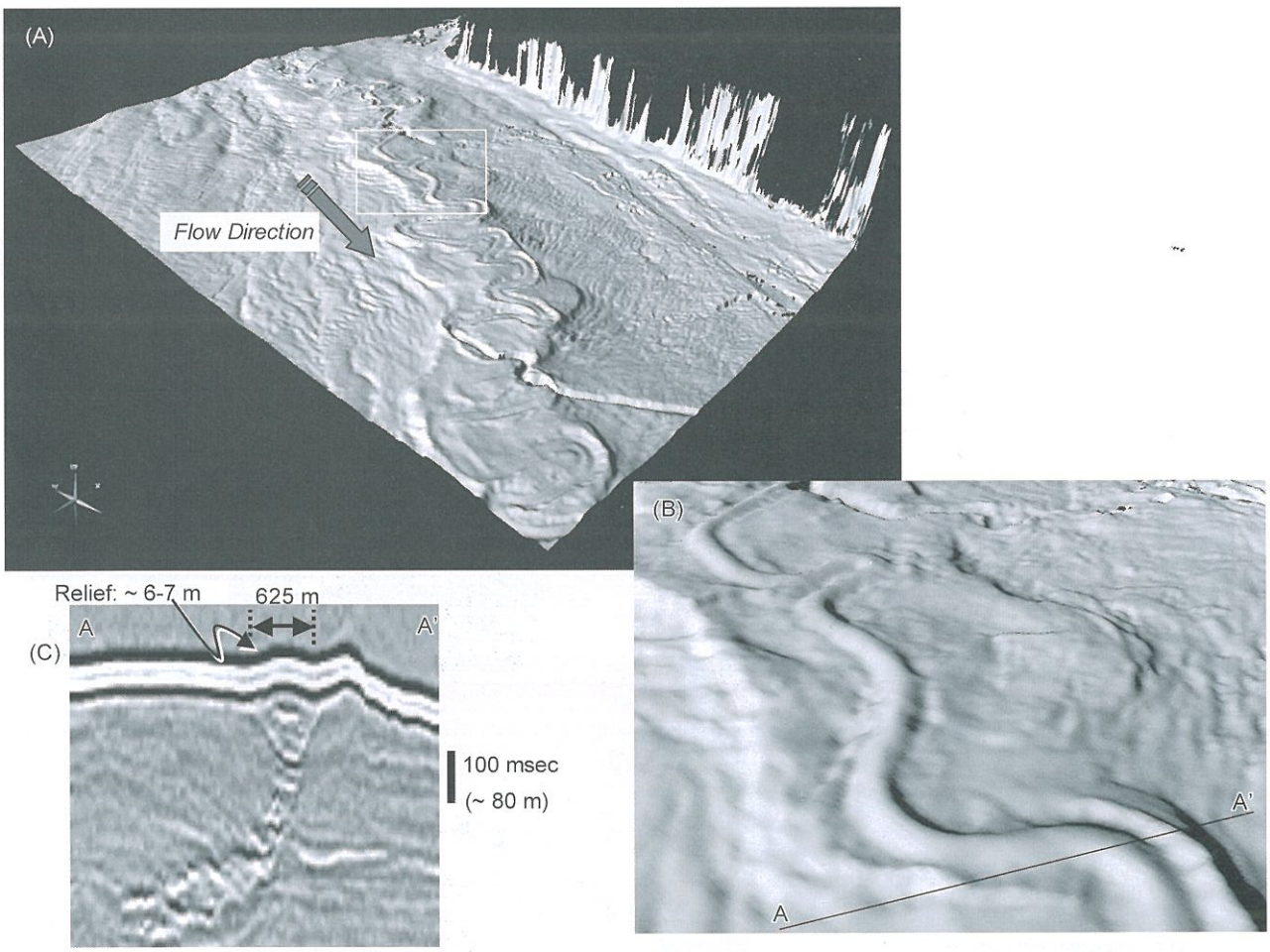

Fig. 18. (**A**) Three-dimensional perspective view of deep-water leveed channel system, eastern Gulf of Mexico. (**B**) Close-up of leveed channel showing effects of differential compaction expressed as channel ridge form. (**C**) Seismic reflection profile transverse to leveed channel flow direction. Channel evolution is characterized by aggradation coupled with lateral migration. The channel fill is characterized by high-amplitude reflections and the post-compaction expression of the channel is that of a ridge form.

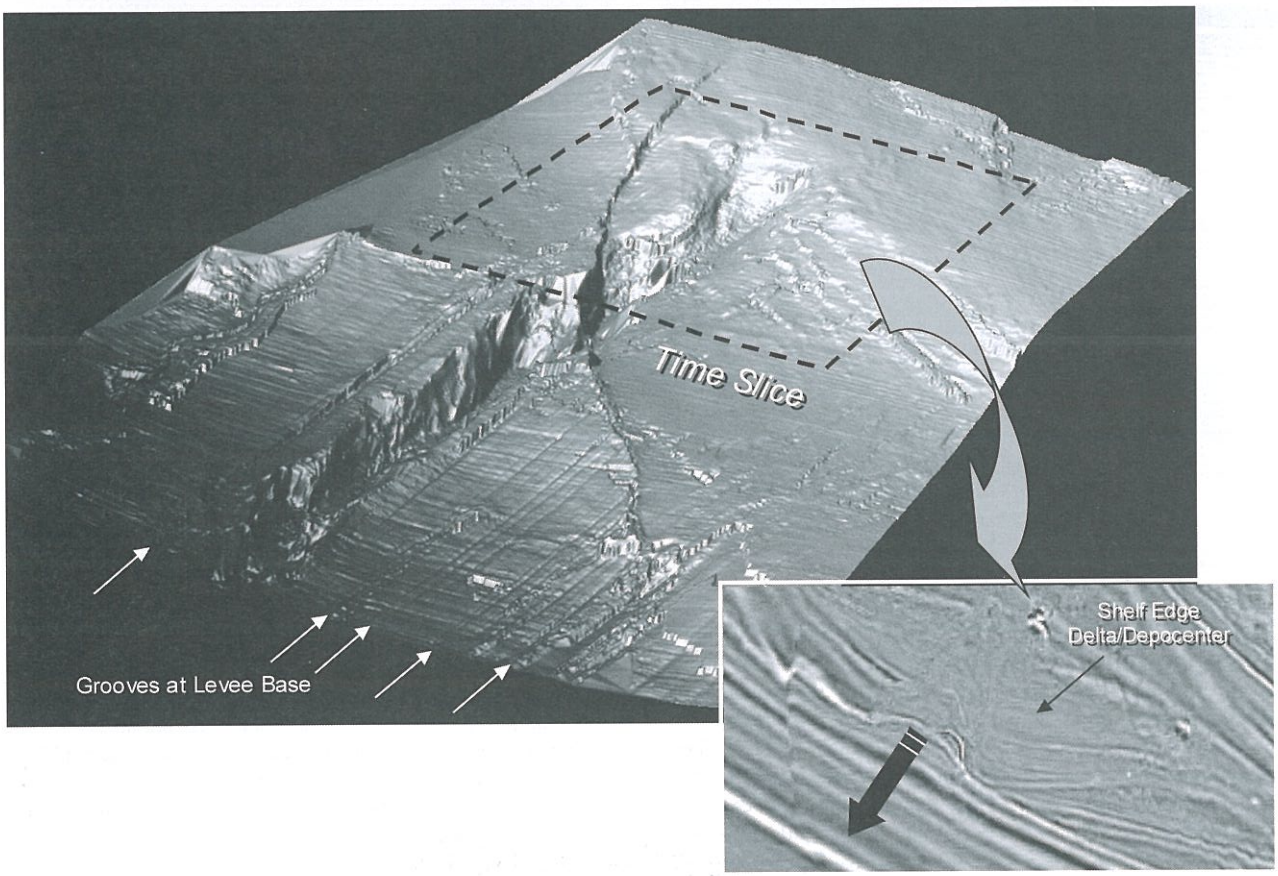

Fig. 19. Three-dimensional perspective view of the outer shelf and upper slope on a surface 80 to 100 m below the sea floor, offshore Louisiana, Gulf of Mexico. The shelf edge and upper slope are shown. The slope is traversed by a channel, which extends inboard of the shelf edge. This inboard extension becomes evident upon examination of the time slice inset. The seaward bulge of the shelf coincides with the position of the slope channel suggesting a genetic link between shelf edge depocenter (i.e. shelf edge delta) and slope channel. The grooves oriented parallel to dip likely were formed by erosion associated with mass transport processes.

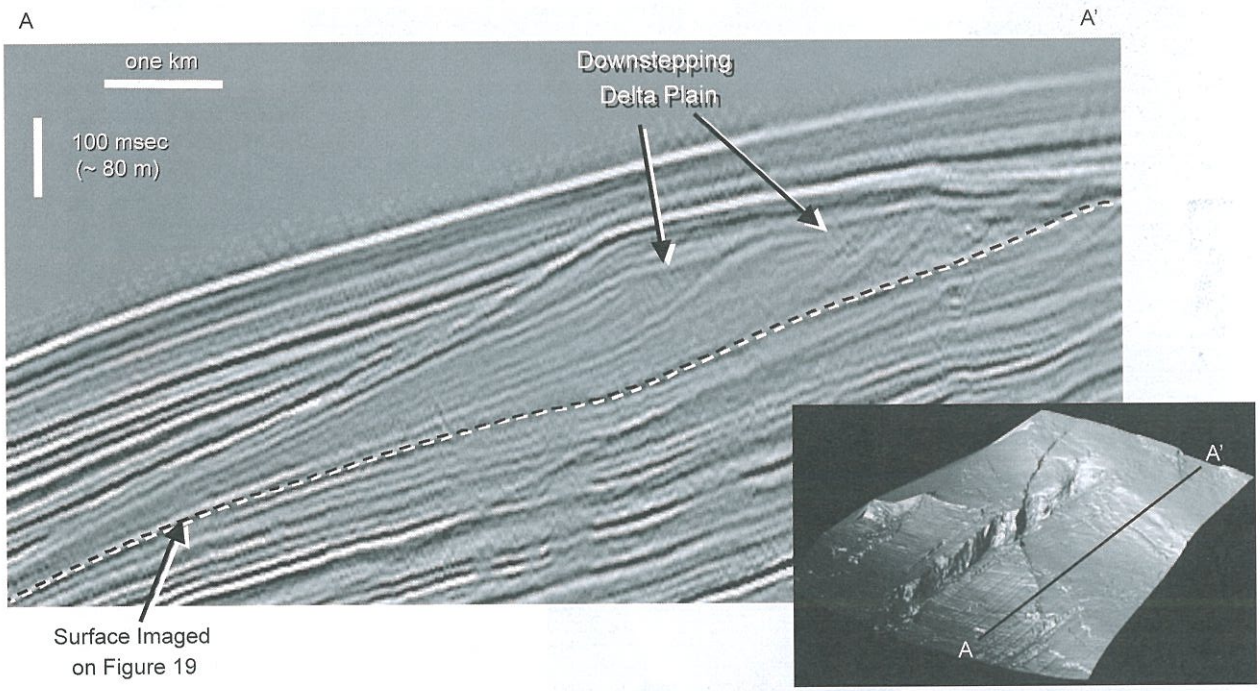

Fig. 20. Dip-oriented seismic reflection profile across the shelf edge delta. The basal part of the delta is characterized by a downstepping delta plain suggesting forced regression and falling relative sea level, and overlain by an aggradational phase in the upper part of the delta suggesting normal regression and rising sea level.

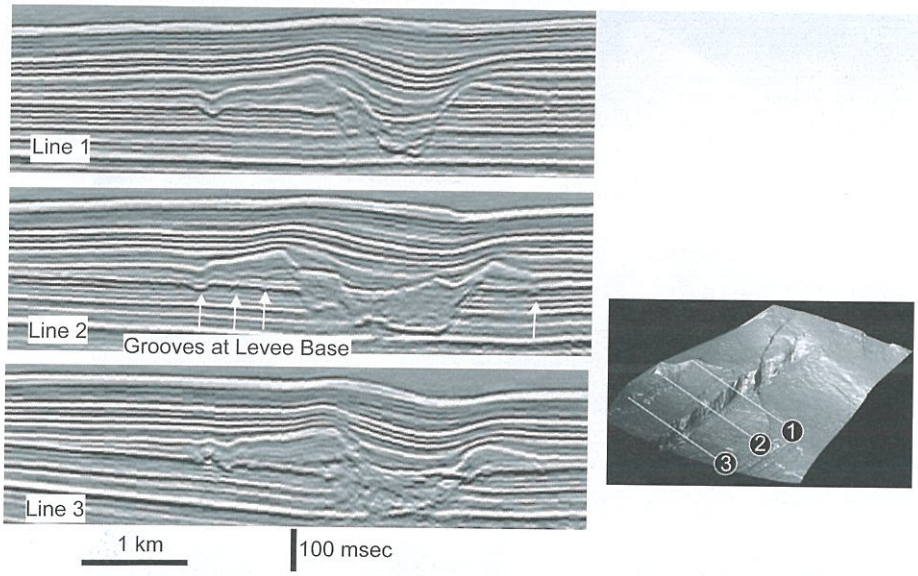

Fig. 21. Transverse seismic reflection profiles across leveed channel imaged in Figure 19. Levee construction can be observed. The grooves on the surface at the base of the levees are annotated on Line 2. The channel base is eroded deeply into the precursor substrate.

channel-levee system that overlies the surface shown in Figure 19. The grooves at the base of these levee deposits likely represent mega-tool marks associated with the passage of slides or debris flows across this surface at the onset of a lowstand depositional episode (Posamentier 2002*b*). The thickness of these levees is as much as twice as great on the right bank (facing down-system) than on the left (Fig. 22) possibly due to the Coriolis force and/or to the Gulf of Mexico loop current.

Shallow-water depositional environments

Shallow-buried shelfal deposits such as shelf edge slump scars and channels, as well as incised valleys, provide useful insights as to what constitute reasonable scales for such features and also provide insights as to which depositional elements tend to be associated with each other. Figure 23 represents a horizon slice at the shelf edge offshore northwest Java, Indonesia. Well-developed slump scars characterize the shelf edge. In addition,

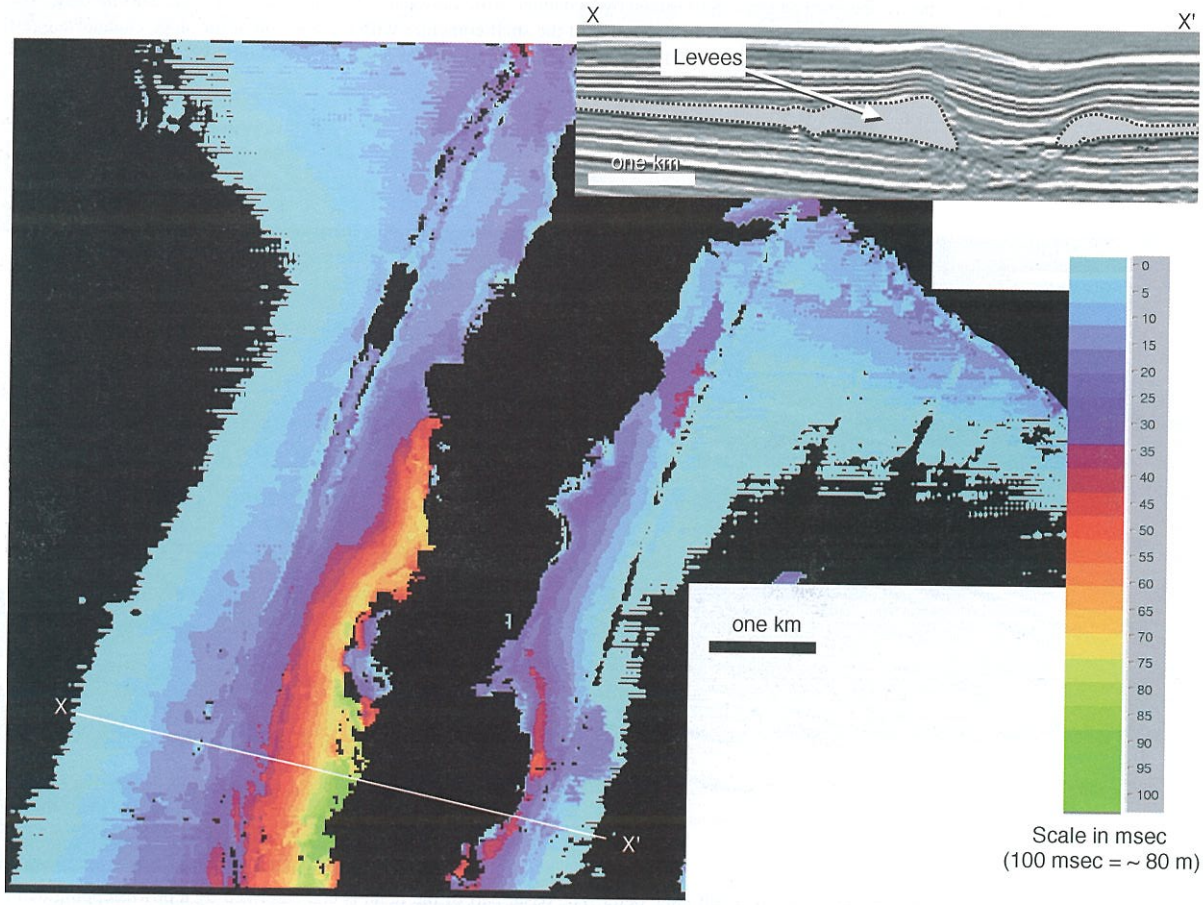

Fig. 22. Isochron map of levee associated with channel imaged in Figure 19. The levee thickness is significantly greater on the west bank, possibly caused by Coriolis force or Gulf of Mexico loop currents.

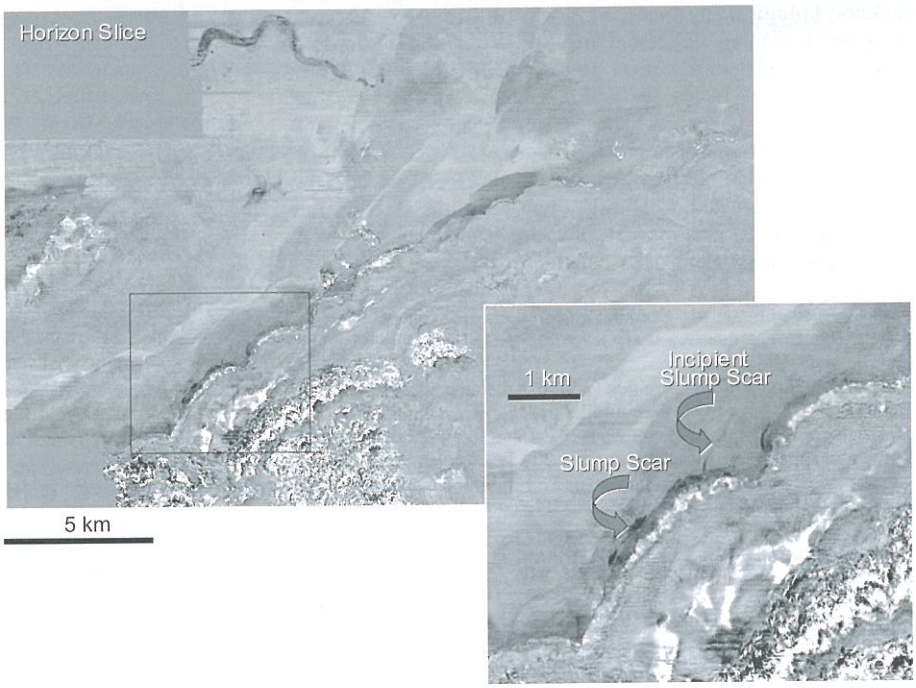

Fig. 23. Seismic horizon slice illustrating outer shelf and upper slope depositional elements offshore Java, Indonesia. Slump scars mark the shelf edge. The inset detail of these slump scars shows incipient slumps located there as well. A small fluvial channel can be observed on the outer shelf.

just inboard of the shelf edge a moderate sinuosity fluvial channel can be observed. On the mid- to inner shelf offshore Java, well developed incised valleys can be observed (Fig. 24). A distinguishing attribute of incised valleys is the presence of associated small tributary incised feeders to the principal channel (Posamentier & Allen 1999). These incised feeder channels suggest the presence of well-drained interfluves that lie above the reach of the river within the trunk valley, even when the trunk river is in flood.

Conclusions

Depositional elements can be observed in plan view images extracted from 3D seismic volumes. The analysis of these features constitutes the study of *seismic geomorphology*. These observations can provide direct as well as indirect benefits to exploration and field development. Where depositional elements can be observed directly at exploration depths, the presence of reservoir, reservoir source, and seal facies can be modelled more accurately. Moreover, the occurrence of stratigraphically defined compartments as well as the potential for stratigraphic trapping of hydrocarbons can be evaluated within the context of the depositional elements identified. Both exploration as well as field development can benefit directly from such analyses.

The indirect benefit derived from seismic geomorphologic analyses derives from examination of shallow-buried features. Shallow-buried features commonly are significantly better imaged than their more deeply buried counterparts. Seismic

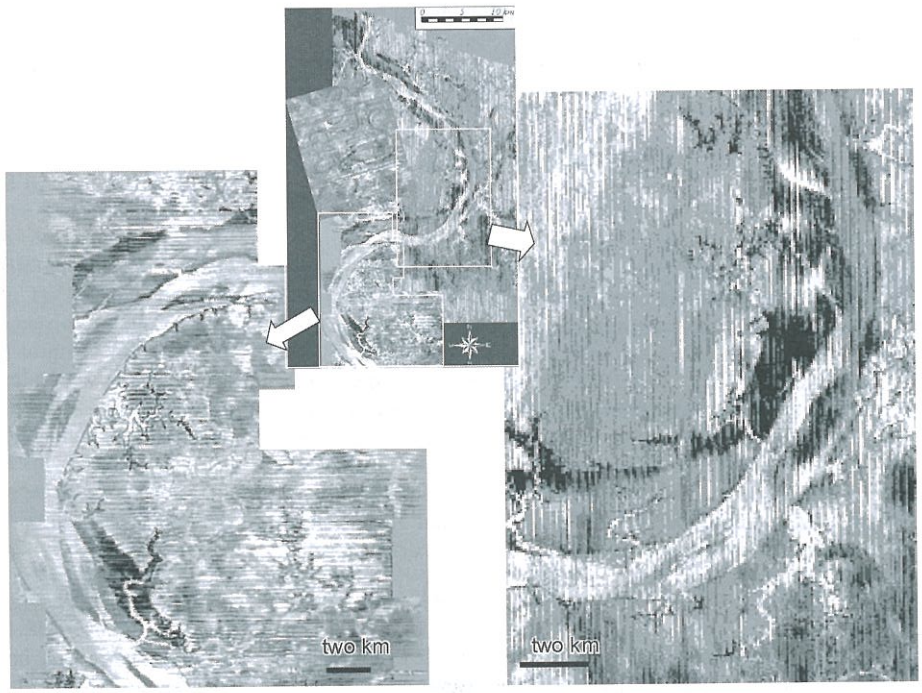

Fig. 24. Incised valley complex offshore northwest Java, Indonesia (Posamentier 2001). Inset details show channel bars, tributary incised valleys and fluvial terraces.

geomorphological analyses of such well-imaged features provide a clearer understanding of depositional element distribution and therefore more accurate prediction of reservoir, source and seal facies. In addition, these analyses enable geoscientists to better evaluate the preservation potential of different depositional elements and therefore the likelihood of encountering such deposits in the ancient rock record. In addition, well-imaged, shallow-buried depositional elements provide 'reality checks' for scale of various such features as well as for depositional element associations.

I thank Anadarko Canada Corporation for permission to publish this paper. Thanks are due Western Geco for permission to publish the seismic data shown in Figures 12–14, 16, 23–24, and to Veritas Exploration Services for permission to publish the seismic data shown in Figures 19–22. In addition I would like to acknowledge the support of R. Evans for his help with data management and interpretation, as well as the user support group at Paradigm Geophysical for their patience and support with regard to my never ending questions regarding the Stratimagic interpretation application. Reviews by T. Garfield, H. Johnson and J. Cartwright were appreciated and helped me in preparation of the final version of this paper.

References

PEAKALL, J., MCCAFFREY, W. D. & KNELLER, B. 2000. A process model for the evolution, morphology and architecture of sinuous submarine channels. *Journal of Sedimentary Research*, **70**, 434–448.

POSAMENTIER, H. W. 2000. Seismic stratigraphy into the next millennium; a focus on 3D seismic data. *American Association of Petroleum Geologists Annual Conference, New Orleans, LA, April 16–19, 2000*, A118.

POSAMENTIER, H. W. 2001. Lowstand alluvial bypass systems: incised vs. unincised. *AAPG Bulletin*, **85**, 1771–1793.

POSAMENTIER, H. W. 2002*a*. Ancient shelf ridges—a potentially significant component of the transgressive systems tract: case study from offshore northwest Java. *AAPG Bulletin*, **86**, 75–106.

POSAMENTIER, H. W. 2002*b*. 3-D seismic geomorphology and stratigraphy of deep-water debris flows. *American Association of Petroleum Geologists Annual Conference, Houston, TX, March 10–13, 2002*, 142.

POSAMENTIER, H. W. & ALLEN, G. P. 1999. Siliciclastic sequence stratigraphy—concepts and applications. *Society of Economic Paleontologists and Mineralogists Concepts in Sedimentology and Paleontology*, **7**, 210p.

POSAMENTIER, H. W., MEIZARWIN, WISMAN, P. S. & PLAWMAN, T. 2000. Deep water depositional systems—Ultra-deep Makassar Strait, Indonesia. *In*: WEIMER, P., SLATT, R. M., COLEMAN, J., ROSEN, N. C., NELSON, H., BOUMA, A. H., STYZEN, M. J. & LAWRENCE, D. T. (eds) *Deep-Water Reservoirs of the World, Gulf Coast Section Society of Economic Paleontologists and Mineralogists Foundation 20th Annual Research Conference*, 806–816.

VAIL, P. R., MITCHUM, R. M. JR. & THOMPSON, S. III 1977. Seismic stratigraphy and global changes of sea level, part 3: relative changes of sea level from coastal onlap. *In*: PAYTON, C. E. (ed.) *Seismic Stratigraphy—Applications to Hydrocarbon Exploration*. American Association of Petroleum Geologists Memoir, **26**, 63–81.

WEIMER, P. & DAVIS, T. L. 1996. *Applications of 3-D Seismic Data to Exploration and Production*, American Association of Petroleum Geologists Studies in Geology, **42**, SEG Geophysical Development Series, No. 5.